Desalination and Water Treatment
www.deswater.com
doi: 10.5004/dwt.2021.26650

214 (2021) 95–106
February

Multi-response factorial design optimization of organic acid separation process using electrodialysis with bipolar membrane

Adam Andrzejewski, Mateusz Szczygiełda, Krystyna Prochaska*

Institute of Chemical Technology and Engineering, Poznan University of Technology, Berdychowo str.4, 60-965 Poznań, Poland, email: krystyna.prochaska@put.poznan.pl (K. Prochaska)

Received 02 March 2020; Accepted 31 May 2020

ABSTRACT

Linear regression and desirability function methodology were employed to optimize the multi-response electrodialysis process with the bipolar membrane (EDBM) for separation of alpha-ketoglutaric acid (AKG) from the post-fermentation broth. A two-level three-factor full factorial design was used to investigate both the main effects and interaction effects of current density, the initial mass of AKG in diluate solution, and volume ratio of the concentrate to the diluate on a set of four system's outcomes. The following system's responses: current efficiency, energy consumption per 1 kg of AKG, the flux of anions through the anion-exchange membranes, and duration of the process were chosen in order to take into account the cost-effective aspect of the EDBM process. According to optimization of the process conditions, the highest effectiveness was obtained for the current density equal to 87.121 A/m^2, 22.5 g of AKG in the diluate chamber at the beginning of separation, and volume ratio of the concentrate to the diluate equal to 0.75. The validation of the simulated EDBM process results was carried out using the model and the actual post-fermentation broth, and the difference between computational and experimental results was 12% or less. Moreover, the coefficient of determination R^2 for every fitted first-order regression model reached over 0.99, which indicates an excellent description of the EDBM process by the collected data.

Keywords: Full factorial design; Optimization; Bipolar membrane electrodialysis; Alpha-ketoglutaric acid; Post-fermentation broth

1. Introduction

The growing importance of the electrodialysis employing the bipolar membrane (EDBM) process is related to the possibility of removal of ionic species from water solutions and electro-acidification in one step [1,2]. It is known that by applying a suitable constant electric field, it is possible to drive migration of cations and anions toward appropriate electrodes. On the other hand, the bipolar membrane (BPM) (which consists of a cation- and an anion-exchange layer) generates hydrogen and hydroxyl ions as a result of water splitting in the thin intermediate layer [3]. Having the above in mind, the BPM has been used for organic acid separation from the actual or model post-fermentation broth and its purification [4–10]. Although the use of electrically-driven membrane techniques is well-documented, the improvement and optimization of these processes have not received due attention. A factorial design is a popular design-of-experiments method based on a statistical approach. This methodology is used to establish the influence of independent variables (factors), determined at fixed levels, on one or more dependent variables (outcomes) [11]. The factorial design allows investigation of

* Corresponding author.

both the main effect and the interaction effect, which is the most significant advantage when compared to the one-factor-at-a-time approach [12,13]. Typically, experimental design methods are applied to improve the process yield or reduce development time and overall cost [13]. Moreover, the factorial design is used as a foundation of the process optimization and modeling.

The design-of-experiment methods have been employed in different branches of science and industry. The first statistical design was proposed by Fisher in the 1920s during his work at the Rothamsted agricultural experimental station. The factorial design found application in the industry at the beginning of the 1930s, when Box and Wilson developed the response surface methodology (RSM), which is treated as an optimization tool. Experimental design methods were widely exploited in chemical and process engineering over the next 30 y, despite the lack of proper computer software. Proposed by Taguchi in the 1980s, the fractional factorial design was an improvement of the design-of-experiment methods, which enabled expanded factorial experiments [13,14]. The above-mentioned techniques are used nowadays for the development of both laboratory and industrial processes.

Literature provides many papers on a combination of the experimental design methods and electrically-driven membrane separation techniques. The factorial design has been used by van der Ent et al. [15] to develop a large-scale enantiomer separation. Wang et al. [16] have optimized the EDBM process for the one-component gluconic acid solution. In turn, Severo Júnior et al. [17] have evaluated the removal of lactobionic acid from multicomponent mixtures by electrodialysis. Camacho et al. [18] have determined the effect of the process conditions, such as voltage, flow rate, type of ion-exchange membrane, and type of feed water, on the EDM desalination process.

However, so far the electrodialysis with BPM has not been optimized concerning the multiple-response process. Our paper as the first one describes the application of desirability function method for such a separation process. The mathematical model, based on the EDBM process performed for model solutions, was validated by experiment using the actual post-fermentation broth, which is a novelty in comparison to other research. Moreover, the paper provides a detailed investigation of the statistical significance of chosen process parameters, which is an extension and complementation of our previous research.

In the presented study, we removed organic acids from multi-component model solutions and actual post-fermentation broth using electrodialysis with BPM. Alpha-ketoglutaric acid (AKG) was chosen as the model organic acid, due to substantial worldwide interest and its wide application mainly in medicine and pharmacy [19,20]. A two-level three-factor full factorial design was the basis of experimental work and the method allowing analyses of both the main effect and the interactions. We checked the statistical significance of the collected data using the analysis of variance (ANOVA) and performed multiple linear regression for the considered responses. The obtained equations provided the empirical model for EDBM of AKG and were employed to optimize the separation process. Finally, the validation of the EDBM process under optimal condition was carried out using the model and the actual post-fermentation broth.

2. Materials and methods

2.1. Materials

In this study of separation of AKG from the model broth solutions, five organic compounds were used AKG, lactic acid (4 g/L), acetic acid (2 g/L), glucose (0.6 g/L), and ethanol (11 g/L). AKG was used in two concentrations; in four experiments it was 28.125 g/L while in the other four it was 46.875 g/L. The model solutions were prepared using deionized water of conductivity not exceeding 3 μS/cm. All components used for the preparation of model solutions were purchased from Sigma-Aldrich (Poland). The composition of model solutions was determined on the basis of the content of organic compounds present in the actual post-fermentation broth (produced using mixed culture *Bacillus natto* and *Pseudomonas fluorescens*) delivered by the Poznan University of Life Sciences (Poland). Before the EDBM process, the actual post-fermentation broth was subjected to pre-treatment procedure including centrifugation, ultrafiltration (UF) through a tubular ceramic membrane (cut-off 15 kDa) delivered by Tami Industry (France) as well as nanofiltration (NF) through a tubular ceramic membrane (cut-off 200 Da) delivered by Inopor (Germany).

2.2. BPM electrodialysis set-up

In our study, an EDBM stack of 10 pairs of alternately arranged anion-exchange (AEM) (PC 200 D) and BPMs (PC bip) was used as the experimental set-up. The active surface area of each membrane was equal to 207 cm^2, which gave the total surface area of 2,070 cm^2 (for each membrane type) for the proposed configuration. All membranes were provided by PCCell (Germany). The membranes were separated from one another by 0.5 mm spacers. The cathode was made of steel 316, and the anode was Pt/Ir-MMO coated with Ti stretched metal. In each experiment, 0.8 L of broth (model or actual) as the diluate, 0.6 or 0.4 L of AKG solution (1 g/L) as the concentrate and 1 L of sulfuric acid solution (0.3 M) as the anolyte and catholyte were fed to appropriate compartments. In the time of the EDBM process, each working solution (diluate, concentrate, catholyte, and anolyte) was circulated in the batch system. Flow pumps (Argal (Poland)) provided a flow rate of 100 L/h in each compartment. The processes were carried out at 298 ± 2 K and under constant electric field (65 or 115 A/m^2) whose value depended on the factorial design set-up. In the EDBM process, the concentrations of the components, conductivity (the accuracy ±0.01 mS/cm), pH-value (the accuracy ±0.01), temperature (the accuracy ±0.1 K), and volume (the accuracy ±0.02 mL) of the concentrate and diluate solutions were monitored. Detail information about the EDBM setup used in these experiments is given in Szczygiełda et al. [21].

2.3. Analytical methods

Samples of diluate and concentrate solutions collected during the EDBM processes were analyzed using

high-performance liquid chromatography (HPLC) HP Agilent 1100 Series (Germany). Moreover, the HPLC setup was equipped with a separating column Rezex ROA-organic acid H+ (8%), Phenomenex®, an autosampler, RI detector (HP 1047A), interface (HP 35900), and a pump (HP 1050). The flow rate of the eluent solution which was 2.5 mM of sulfuric acid, was equal to 0.6 mL/min, while the temperature of the column, as well as that at the input to the detector, was equal to 50°C, P = 0.2 MPa.

2.4. Calculation

The current efficiency (CE) and the specific energy consumption (EC) were calculated in order to determine the efficiency of the investigated EDBM processes, using the following equations [22,23]:

$$\mathrm{CE} = \frac{F \cdot z \cdot V \cdot \Delta C_{\mathrm{diluate}}}{n \cdot I \cdot \Delta t} \cdot 100\% \tag{1}$$

where CE is the current efficiency (%); F is the Faraday's constant (96,485) (C/mol); I is the current intensity (A); z is the valence of ions; V is the diluate volume (L); $\Delta C_{\mathrm{diluate}}$ is the change of AKG concentration in the diluate chamber (mol/L); n is the number of cell pairs; Δt is the change of time (s):

$$\mathrm{EC} = \int_0^t \frac{U \cdot I}{\Delta m} dt \tag{2}$$

where EC is the specific energy consumption needed to produce 1 kg of AKG (kWh/kg); U is the voltage (V); I is the current intensity (A); Δm is the increment of AKG mass in concentrate solution (g); t is the time (h). The average flux of AKG anions through the membrane was calculated as follows:

$$J_m = \frac{\Delta m}{A \cdot t} \tag{3}$$

where J_m is the average flux of AKG anions through the membrane [kg/(m²h)]; Δm is the increment of AKG mass in concentrate solution (kg); A is the total area of anion-exchange membranes (m²); t is the time (h).

2.5. Experimental design

The statistical computing was performed in RStudio using R language and environment version 3.5.3, which are distributed under the terms of the GNU General Public License. All used packages (janitor, lattice, qualityTools, MANOVA.RM, dplyr, car, and plotly) are available in the comprehensive R archive network (CRAN) package repository. The two-level three-factor full factorial design was employed to study the effects of three independent variables (factors), that is, current density (A), the initial mass of AKG in the diluate solution (B), and volume ratio of the concentrate to the diluate. Each factor was considered at two levels, which were determined according to the method proposed in our previous papers [24–26]. Both coded and actual values of independent variables are presented in Table 1.

It should be added that the volume of the diluate solution was always equal to 0.8 L and the volume of the concentrate solution depended on the level of the factorial experiment: 0.4 L for –1 and 0.6 L for +1.

Four dependent variables were taken into account to ensure a comprehensive analysis of EDBM. Current efficiency and energy consumption describe the cost-effectiveness of the process, while the flux of AKG anions through the anion-exchange membrane and the time of the process determines the rate of electrodialysis. The first-order linear regression model was fitted to each response, but it contained only statistically significant factors and their interactions.

2.6. Optimization set-up

Simultaneous optimization of the obtained equations was performed using the desirability function method proposed by Derringer and Suich [27] and Derringer [28]. Each experimental response value was transformed to desirability value d_i, where $0 \le d_i \le 1$. The value of d_i increases as the "desirability" of the corresponding response increases [27]. The higher the value of current efficiency and the flux of AKG ion through the membranes, the better. The lower the value of energy consumption per 1 kg of AKG, the higher the desirability. Moreover, each response was assigned with a weight that corresponded to its importance (Table 2). The value of weight w_i for each EDBM process response was determined taking into account the cost-effectiveness of the process (equipment cost dependent on solute flux > cost of specific energy > current use > overall process time) [29]. The weighted overall desirability D of the considered system of equations was calculated as follows [28]:

$$D = \left(d_1^{w_1} \cdot d_2^{w_2} \cdot d_3^{w_3} \cdot d_4^{w_4}\right)^{\frac{1}{\sum w_i}} \tag{4}$$

The maximum of function (Eq. (4)) was determined using *optimum* function of qualityTools package. It was necessary to impose constraints on both dependent and independent variables to avoid physically inconsistent results of optimization, for example, a negative value of time. All variables were considered between limits set by the two-level three-factor full factorial design (Table 1) and maxima and minima of the responses.

In this study, two additional EDBM experiments were carried out to validate the obtained model and optimization

Table 1
Levels of independent process variables used in full factorial design

	Factor		
	A	*B*	*C*
Low level (–1)	65	22.5 (28.125)	0.5
High level (+1)	115	37.5 (46.875)	0.75
Name	Current density	Mass	C:D volume ratio
Unit	(A/m²)	(g) ([g/L])	(–)

results. The best process conditions were applied to the model solution of the composition presented in section 2.1 (Materials) and to the pre-treated actual post-fermentation broth.

3. Results and discussion

3.1. Experimental

In the first part of our investigation, eight unique EDBM processes of AKG separation from model solutions were conducted following 2^3 full factorial design methodology. Each separation for the model post-fermentation broth was replicated. Experiments were carried until reaching a conductivity of 2.5 mS/cm in diluate solution, which corresponded to the recovery of AKG in over 95% of the initial mass. This relationship was determined experimentally before the investigation presented in this paper (data not shown). The obtained curves group in pairs according to the same value of current density and initial mass of AKG in diluate solution (Fig. 1) which results in almost the same duration of the acid separation in such processes. One can conclude that a change of volume ratio of the concentrate to the diluate (factor *C*) shows no influence on the process duration. The above-mention tendency and the conditions of ending the experiment (conductivity lower than 2.5 mS/cm) are illustrated in Fig. 1.

Experimental results are presented in Table 3 and Fig. 2 in the form of a bar chart. Original values were min-max normalized, which means the minimum of the response value is obtained when a bar reaches 0, and the maximum is achieved in 1. The highest value of current efficiency (75.72%) was reached for the process coded as *C*, which corresponds to the high value of volume ratio of the concentrate to the diluate. Such a result followed from the slower rise of AKG concentration in the concentrate solution, which indicated a slower increase in the undesirable backward diffusion in comparison with high-mass processes [30]. On the other hand, the lowest value of current efficiency (69.49%) was obtained when the initial mass of AKG in diluate solution (*B*) was high, and the other factors remained at low levels. The concentration of AKG in the concentrate chamber raised fast because of the low volume of the concentrate, which resulted in a decrease in CE caused by the concentration polarization effects [31].

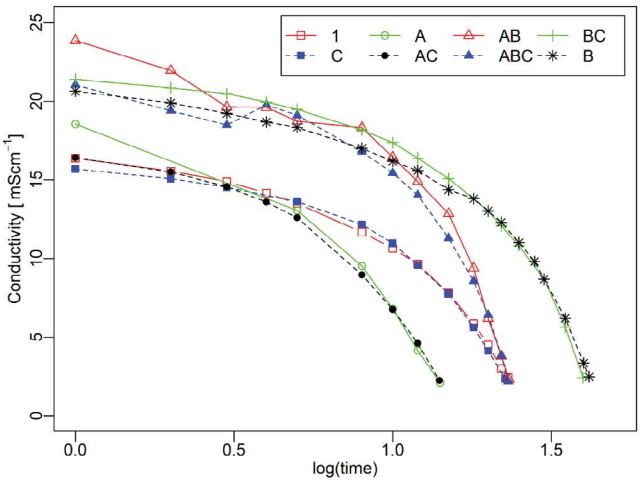

Fig. 1. Conductivity – log(time) curves of factorial design experimental runs. Legend explanation – a presence of factor coding letter indicates a high level of this factor.

Table 2
Optimization details

Response	Target	Weight (1–10)	Lower bound	Upper bound
Current efficiency (%)	Maximize	6	69.49	75.72
Energy consumption (kWh/kg)	Minimize	8	0.327	0.515
Flux (kg/(m^2 h))	Maximize	10	0.256	0.463
Time (min)	Minimize	4	13.99	42.10

Table 3
Results of full factorial design EDBM experiment

Exp. mark	Factor			Current efficiency (%)		Energy consumption (kWh/kg)		Flux (kg/(m^2 h))		Time (min)	
	A	*B*	*C*								
1	–1	–1	–1	73.27	73.40	0.340	0.339	0.272	0.275	23.28	23.10
A	1	–1	–1	70.91	70.65	0.507	0.509	0.448	0.444	13.99	14.11
B	–1	1	–1	69.49	69.53	0.358	0.356	0.256	0.262	42.10	41.62
AB	1	1	–1	72.76	72.51	0.484	0.489	0.462	0.457	23.25	23.38
C	–1	–1	1	75.72	75.63	0.329	0.327	0.282	0.283	22.62	22.84
AC	1	–1	1	71.80	71.63	0.503	0.515	0.454	0.455	14.05	14.14
BC	–1	1	1	72.09	71.92	0.346	0.343	0.268	0.269	39.80	39.78
ABC	1	1	1	73.23	73.06	0.481	0.486	0.463	0.460	23.12	23.16

The flux of AKG anions through the anion-exchange membrane reached high values for experiments *A*, *AB*, *AC*, *ABC*, which corresponded to the high level of current density. This relationship, also observed by Mier et al. [32], indicates the dominant role of electric driving-force on the flux through the membrane over the diffusion one [33]. Such a correlation was observed even for the experiments with the high initial mass of AKG in the diluate chamber (*AB*, *ABC*), in which a greater backward diffusion should be observed, as mentioned above. Probably, the effect of strong electric field overcame the back diffusion-driven flux and minimalized its contribution to the overall transport through the membranes.

In contrast to the flux, the high value of current density negatively affects the energy consumption per 1 kg of AKG. The higher the electric current, the more energy is used [32], so the highest value of EC was achieved for the same processes as for the flux of AKG ions. The lowest value of energy consumption corresponds to the highest value of current efficiency, so the explanation of this case is analogous.

The duration of the electrodialysis process with bipolar membrane (EDBM) is related to two effects. One the one hand, the time of process decreased with rising current density, but on the other hand, it increased with the growth of the initial mass of AKG in diluate solution. The shortest separation process (13.99 min) was achieved for the process coded as A, because of the highest driving-force produced by current density and the slowest rise of backward diffusion. The longest process (42.10 min) was the one with the highest initial mass of AKG in diluate solution (*B*), which indicates that the greater the mass that has to be transported, the longer the separation process.

Each response related to the driving-forces, that is, current efficiency, the flux of AKG anions through the anion-exchange membrane and time, can be well-explained in terms of the Nernst–Planck (N–P) equation, which is the phenomenological description of the ion diffusion transport through the membrane caused by both concentration difference and electric migration [32]:

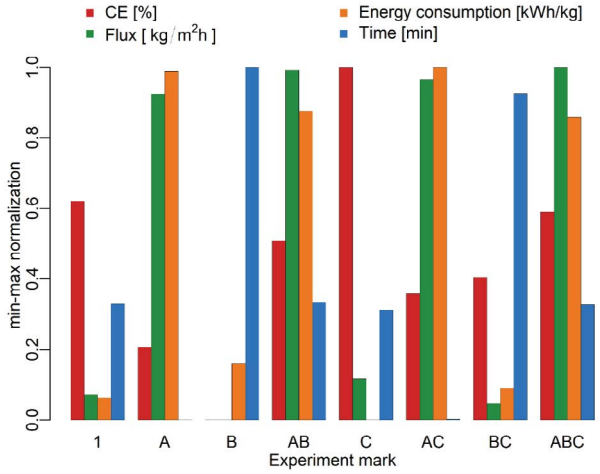

Fig. 2. Bar plot of minimum–maximum normalized process responses.

$$J_i = -D_i \frac{dC_i}{dy} + \eta \frac{z_i F C_m D_i}{RT} \frac{d\varphi}{dy} \tag{5}$$

Eq. (5) is the reduced form of N–P equation because the ion-exchange membranes are non-porous, so the term describing the convective transport could be neglected [32]. The first part of Eq. (5) is interpreted as the diffusion transport dependent on the value of concentration difference between concentrate and diluate chambers. The second part of Eq. (5) describes the migration caused by an electric field which depends on the potential gradient. During the EDBM process, the concentration gradient changes, but the electrical potential difference remains steady. At the beginning of AKG separation, a high concentration in diluate solution and low concentration in concentrate solution generate an additional flux which combines with migration and ensures fast transport of AKG ions. However, the longer the process, the weaker the diffusion and finally, when the concentration of AKG in both chambers is the same, the diffusion starts affecting the EDBM process in a negative way. The strength of backward diffusion increases, extending the process, which effects the values of CE, EC, and flux through the anion-exchange membranes.

3.2. Linear regression model

The collected data were analyzed using ANOVA, which allowed determination of the statistical significance of the main effect and interactions of factors on the level of significance equal to 0.05. Then, the linear regression models were fitted respecting only significant values of the main effect and interaction of factors. The generated results are shown in Table S1 and the proposed regression equations for the appropriate non-coded form of the considered variables are presented below (Eqs. (6)–(9)):

$$\begin{aligned} \mathrm{CE} &= 83.32 - 1.532 \cdot 10^{-1} A - 7.168 \cdot 10^{-1} B + 18.46C \\ &\quad + 7.555 \cdot 10^{-3} AB - 1.176 \cdot 10^{-1} AC + 5.915 \cdot 10^{-4} ABC, \\ R^2 &= 0.995; \end{aligned} \tag{6}$$

$$\begin{aligned} \mathrm{EC} &= 2.106 \cdot 10^{-1} + 2.670 \cdot 10^{-3} A - 1.095 \cdot 10^{-1} C \\ &\quad - 5.897 \cdot 10^{-6} AB + 9.389 \cdot 10^{-4} AC, \\ R^2 &= 0.998; \end{aligned} \tag{7}$$

$$\begin{aligned} \mathrm{Flux} &= 1.348 \cdot 10^{-2} + 3.660 \cdot 10^{-3} A + 2.841 \cdot 10^{-2} C + 9.357 \cdot 10^{-7} AB, \\ R^2 &= 0.999; \end{aligned} \tag{8}$$

$$\begin{aligned} t &= -19.29 + 1.62550 \cdot 10^{-1} A + 2.515367 B + 16.036C - 1.6247 \cdot 10^{-2} AB \\ &\quad - 1.26400 \cdot 10^{-1} AC - 9.11200 \cdot 10^{-1} BC + 7.413 \cdot 10^{-3} ABC, \\ R^2 &= 0.999; \end{aligned} \tag{9}$$

The coefficient of determination R^2 for all fitted models is higher than 0.99, which indicates an excellent description of the experimental data by the regression equations.

3.3. Main effects

Detailed investigation of the main effects which allowed determining the averaged effect of each independent variable on each response is presented in Fig. 3. The obtained effect plots confirmed the variance analysis results as they indicated the same factors as insignificant.

According to Fig. 3 and ANOVA (Table S1), the current density influenced each outcome. Current efficiency decreased with increasing current density, which could be explained by more effective generation of hydroxyl anions that compete with AKG anions [34] and an increase in consumption of energy to overcome the electrical resistance [35]. It should also be noted that when the high current density is applied, an increase in water transport induced by the electro-osmosis effect can be observed [21]. The above-mentioned reasons also explain the rise of energy consumption per 1 kg of AKG, because less electric current is converted into the desired product, so much more energy is needed to transport the same quantity of AKG ions through the anion-exchange membranes [32]. The influence of current density on the flux and duration of the process were presented in section 3.1 (Experimental).

The effect of increase in the initial mass of AKG on current efficiency was discussed above, although some more explanation is needed. As mentioned above, the drop of CE was caused by the rise of AKG concentration in concentrate solution, which resulted in the backward diffusion of ions. A similar observation has been made in our previous paper [34] for fumaric acid EDBM process. Furthermore, in the cited paper, we have suggested the formation of a polarization layer at the membrane surface, which generates a concentration gradient in the diluate compartment [34]. Such a mechanism is also possible in the separation of AKG in the EDBM process. The effect of initial mass in diluate solution on the energy consumption and flux of ions through the membrane was at a level of statistical error and according to the conducted ANOVA (Table S1), it can be neglected. The duration of the separation process increased with increasing initial mass of AKG in the diluate chamber because the EDBM yield is limited by transporting capacity of the membranes. Moreover, the long time of the process can be explained by the effect of backward diffusion which extended the proceeding, especially for low current density separations.

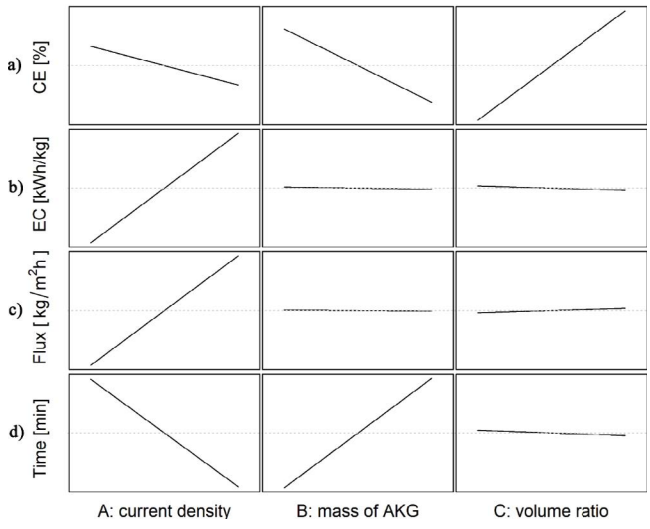

Fig. 3. Main effects plots for (a) current efficiency, (b) energy consumption per 1 kg of AKG, (c) flux of AKG anions through the membranes, and (d) time of the EDBM process.

The current efficiency was observed to increase with increasing volume ratio of the concentrate to the diluate. The high volume of concentrate solution implies a slower rise of AKG concentration, which permitted maintaining positive diffusion flux for a longer time. The *C:D* ratio also had a significant effect on the other EDBM responses (Table S1), but according to the main effects plot (Fig. 3), the change in each response value is meagre comparing to the other described effects. After the main effects analysis, one can anticipate that the current density is the most crucial factor for investigated separation of AKG using the EDBM technique.

3.4. Interaction effects

The interaction plot (Fig. 4) shows a relationship between the independent variables and permits finding if the effect of one factor on the EDBM outcome depends on the state of another factor. Each two-way combination of two-level three-factor full factorial design for the EDBM process of AKG separation is considered and presented in Fig. 4.

As far as current efficiency is concerned, there are interactions *AB* and *AC*, which are also proved by ANOVA (Table S1). For a low level of current density, the rise of the initial mass of AKG in the diluate chamber from 22.5 to 37.5 g resulted in a drop of CE but for a high level of current density, the change in the level of factor *B* from –1 to +1 caused an increase in CE. These observations prove the theory that for fixed initial mass, the contribution of diffusion to the transport flux remains steady, and the part of electric driving-force used to overcome the backward diffusion decreases when the current density rises. As far as the *AC* interaction is concerned, the effect of higher volume in the concentrate chamber was stronger for the low-current EDBM process, when compared to that in the high-current EDBM process. Also, when the separation process is conducted under a high current density, the participation of diffusion in the flux through the anion-exchange membranes becomes less significant. Regardless of the levels of factor *C*, the lines referring to different initial masses of AKG in diluate solution, remain parallel, which means that the effect of factor *C* is independent of the level of factor *B*.

Similarly to CE, there is the interaction between the current density and the initial mass of AKG in the diluate chamber (*AB*) for the energy consumption of the EDBM process. Moreover, an analogous explanation of this interaction can be given, which was also highlighted in section 3.1 (Experimental). The interaction *AC* shows that regardless of the level of the initial mass of AKG in diluate solution, the EC remained steady for the current density equal to 115 A/m^2 (*A* = +1), which is a really interesting feature of the investigated process. On the other hand, when factor *A* was considered at the level coded as –1, the energy consumption dropped slightly, when factor *C* was changed

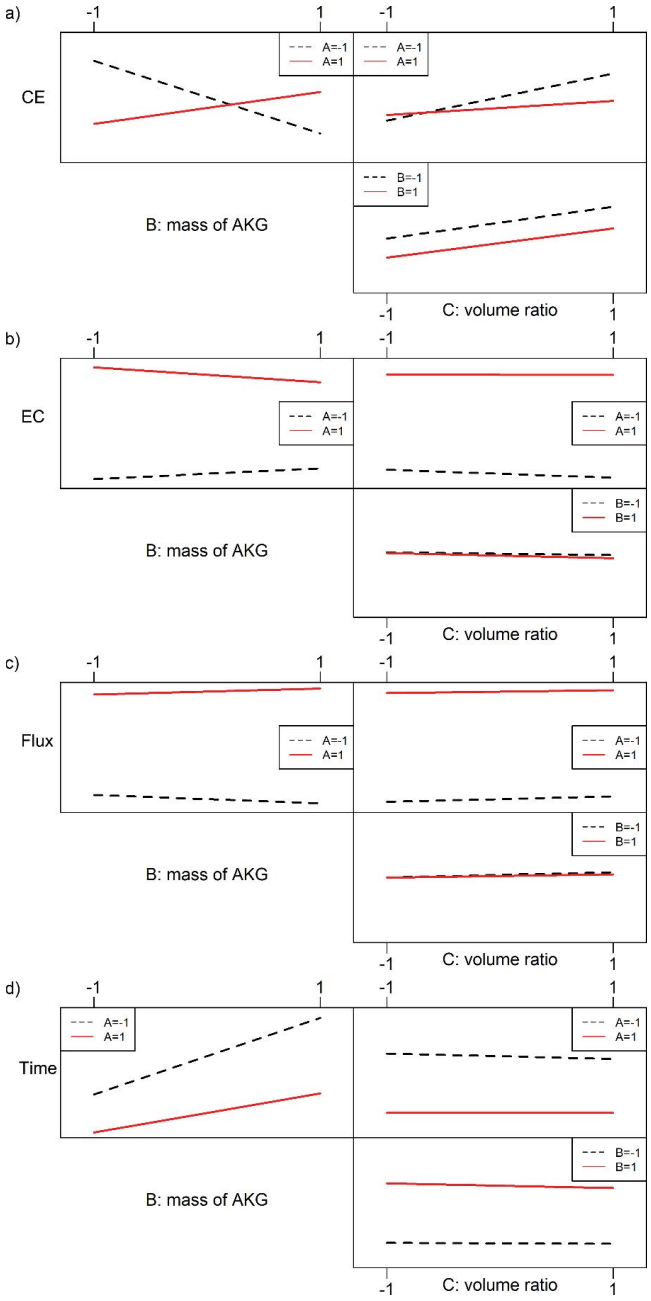

Fig. 4. Interactions plots for (a) current efficiency, (b) energy consumption per 1 kg of AKG, (c) flux of AKG anions through the membranes, and (d) time of the EDBM process.

from the low level to the high one. Again such a phenomenon confirms that the diffusion transport contributes to the total flux of ions through the membranes to a greater extent for low-current processes, which was also observed in the effects plot (Fig. 3). The interaction *BC* is not statistically significant according to the ANOVA (Table S1).

In contrast to the effect of combinations of the other factors on the flux of AKG ions, the interaction between the current density and the initial mass of AKG in the diluate chamber was found statistically significant according to ANOVA (Table S1). For factor *A* at the high level, the increase in *B* contributed to the rise of anion flux, but for the lower value of current density, the effect of *B* increase was reverse. High current density value brings about a reduction of EDBM time, which results in shorter exposure of AKG anions flux to backward diffusion and lower contribution of diffusion transport in the total transport, as mentioned above. For both levels of current density, the duration of the EDBM process increased, when the initial mass of AKG in diluate chamber was higher, but the growth was more considerable for the low level of factor *A*. It is another example of the driving-force influence on the process responses. The low-current process ($A = -1$) must consume a greater part of the electric migration transport flux to overcome backward diffusion. Similarly, the diffusion contribution was observed for *AC*, for which the lines corresponding to different levels of current density are almost parallel (Fig. 4), but the *AC* interaction is statistically significant (Table S1). For the low level of factor *A*, with increasing volume of concentrate solution, the time of the EDBM process was reduced, however, for the high level of factor *A*, the time duration remained unchanged. The higher ratio of the chambers' volumes implies longer time of the positive diffusion flux and lower backward diffusion effect because it inhibits the fast rise of AKG concentration in concentrate solution. For both levels of the initial mass of AKG in diluate solution, the change in factor *C* from –1 to +1 caused a slight decrease in the EDBM duration, but the effect was greater for the high-mass processes. Such an observation can be explained by the greater contribution of the diffusion flux to the total transport capability when the initial mass of AKG is higher. The processes in which the diffusion plays an important role are sensitive to dilution, which was mentioned earlier in this paper.

Moreover, the proposed model also takes into account the three-way interaction between the factors, although it seems to be too complicated for interpretation and too difficult for graphic presentation.

3.5. Optimization

Finding the optimal process conditions for one dependent variable is an effortless issue, and the best EDBM process parameters can be specified without any shadow of a doubt. The situation becomes much more complicated when it comes to taking into account more than one dependent variable. None of the presented experiments (Fig. 2) simultaneously provided the maximal values of current efficiency and flux of AKG anions through the anion-exchange membrane and the minimum energy consumption and experiment duration. Such a case requires multivariable optimization.

The optimization was conducted using the desirability function methodology, in which the experimental data were normalized in the range from 0 to 1, and the best direction to maximize the desirability function was found. The single-response desirability followed the targets and constraints presented in Table 2 and surface plots for each EDBM response are shown in Fig. 5. The presented plots are prepared for the averaged value of both levels of volume ratio of the concentrate to the diluate. Both the current efficiency and the energy consumption per 1 kg of AKG desirabilities

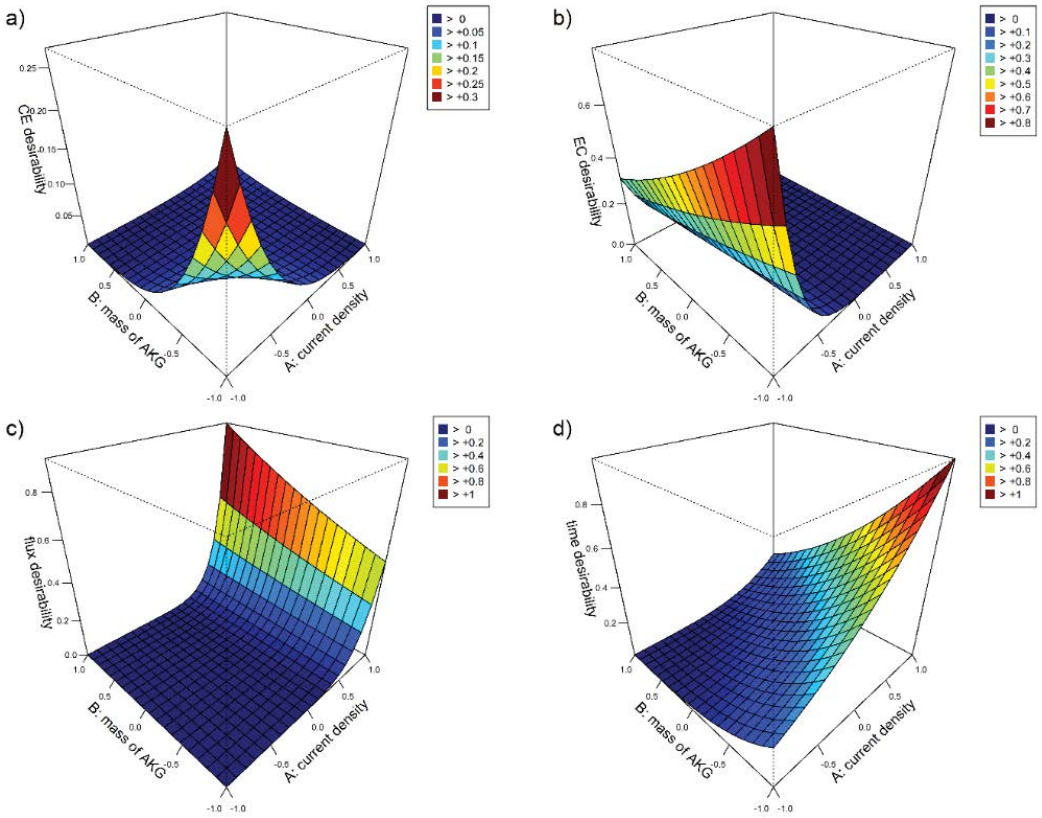

Fig. 5. Single desirability surface plots for (a) current efficiency, (b) energy consumption per 1 kg of AKG, (c) flux of AKG anions through the membranes, and (d) time of the EDBM process.

match the best values for the low levels of factors *A* and *B*. The flux is maximized for the high level of each independent variable but time is optimal for the higher value of the current density and the lower value of the initial mass of AKG in diluate solution. Simultaneous investigation of the multivariable system of equations produced another surface plot interpreted as composed desirability of investigated EDBM separation of AKG and shown in Fig. 6.

The optimization involved finding maximum of the function obtained, which surely falls at the lower value of the initial mass of AKG in diluate chamber and somewhere between the low and the high value of current density. The probable optimal value of factor *C* cannot be specified according to Fig. 6, but the optimization was made taking into account all dependent variable regression models (Eqs. (6)–(9)), so the volume ratio of the concentrate to the diluate was also considered.

Both the optimal process factor combination and simulated values of responses are presented in Table 4. The best EDBM process conditions are obtained for the current density equal to 87.121 A/m^2, 22.5 g of AKG in the diluate chamber at the beginning of separation, and the volume ratio of the concentrate to the diluate equal to 0.75.

As mentioned in section 2.1 (Materials), the optimal factor composition was validated by two additional EDBM processes, one for the model solution and another for pretreated actual post-fermentation broth. A comparison of experimental results with simulated ones is shown in Fig. 7. The current efficiency is the highest for the simulated process; the lowest for the actual post-fermentation broth and the value for the model solution is intermediate. The energy consumption per 1 kg of AKG is greater for broth and almost the same for the other compared data sets. The flux of AKG anions through the anion-exchange membranes reaches the highest value for the simulation; the smallest value for the broth and an intermediate value for the model solution. The EDBM process lasts the longest for the actual post-fermentation broth and a little bit shorter for the simulation. The time of AKG separation is the shortest for the model solution, which does not match the pattern of the other responses. All differences between the simulated data and the model solution results can be explained by an imperfection of regression models and experimental errors. Any response value for the actual post-fermentation broth is worse than for the simulated values (maximally about 12% for the flux of AKG anions through the membranes) and model solution (maximally about 4% for the flux of AKG anions through the membranes) results in respect to the optimization targets (Table 2). Such behavior is caused by a much more complex composition of fermentation broth. For example, the presence of inorganic ions leads to a decrease in the EDBM efficiency because of the competition for transport through the AEM with much larger and less mobile in the electric field AKG anions. A similar relationship has been observed in our previous study during the separation of succinic acid from the fermentation

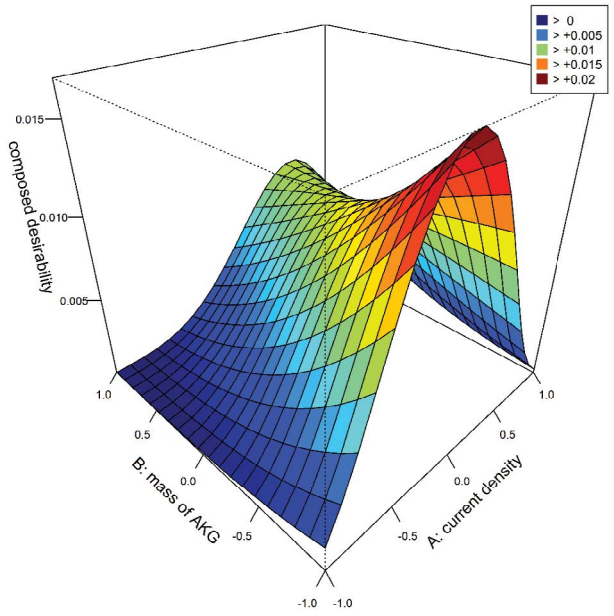

Fig. 6. Overall desirability surface plot.

broth left-after biodiesel production [21]. Nevertheless, the obtained models and optimization method are good enough to simulate the EDBM process of AKG separation.

4. Conclusion

The 2^3 full factorial design carried out in our study allowed investigation of both main effects and the interaction effects of the current density, the initial mass of AKG in the diluate solution, and volume ratio of the concentrate to the diluate for electrodialysis with the BPM. The highest impact on each outcome had the current density points to the importance of transporting driving-forces. The contribution of diffusive transport to the total flux of anions through the anion-exchange membranes differs from the value of electric migration represented by current density. For low values of current density, the diffusion and backward diffusion stronger influence the overall transport.

Factorial design experimental data were used to perform linear regression and propose a model of EDBM process for AKG separation. The obtained system of equations has been optimized taking into account the assumed targets and constraints. On the basis of the desirability function

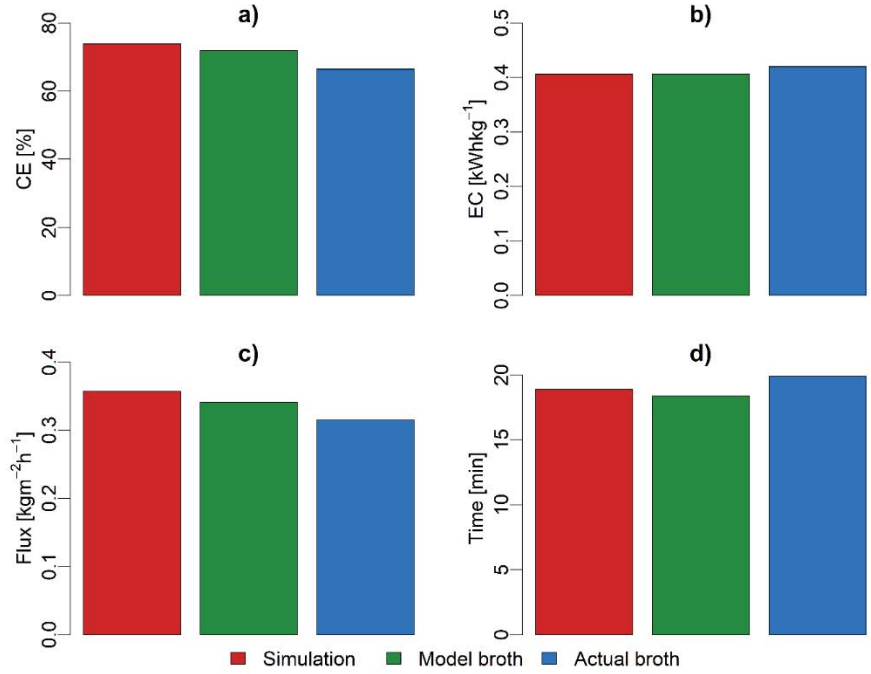

Fig. 7. Comparison of simulated data with model solution EDBM process and actual post-fermentation broth EDBM process for (a) current efficiency, (b) energy consumption per 1 kg of AKG, (c) flux of AKG anions through the membranes, and (d) time of EDBM process.

Table 4
Results of optimization and predicted values of responses

	Current efficiency (%)	Energy consumption (kWh/kg)	Flux (kg/(m^2 h))	Time (min)	Overall desirability		Factor		
							A	*B*	*C*
Response	73.89	0.406	0.357	18.91	0.597	Coded	–0.115	–1	1
Desirability d_i^{wi}	0.124	0.0127	0.000738	0.463		Real value	87.121	22.5	0.75

methodology, it was found that the best EDBM factors set was: current density equal to 87.121 A/m^2, 22.5 g of AKG in the diluate chamber at the beginning of separation, and volume ratio of the concentrate to the diluate equal to 0.75. The values of the predicted responses for optimal separation conditions were verified using the model and the actual post-fermentation broths. The differences between simulated data and those obtained for the model solution and post-fermentation broths (not bigger than 4% and 12%, respectively) were caused by a much more complex composition of the actual post-fermentation broth, for example, the presence of inorganic ions which competed in transport through the AEM with AKG anions.

As was shown, the determination coefficient R^2 for every fitted first-order regression model reached over 0.99. Thus, the obtained results indicate an excellent description of the EDBM process by the collected data. However, in our further research, we are going to employ more complex factorial designs to investigate the fit of higher-order regression equations to obtained experimental data.

Acknowledgments

The authors wish to acknowledge the financial support from the National Science Centre, Poland (Grant no. 2017/25/N/ST8/00963). We are also much grateful to D.Sc. Daria Szymanowska-Powałowska from the Poznan University of Life Sciences, Poland, who kindly provided us with the post-fermentation broth.

Abbreviations

A	—	Factor interpreted as current density
AB	—	Interaction between factors *A* and *B*
ABC	—	Interaction between factors *A*, *B*, and *C*
AC	—	Interaction between factors *A* and *C*
AEM	—	Anion-exchange membrane
AKG	—	Alpha-ketoglutaric acid
ANOVA	—	Analysis of variance
B	—	Factor interpreted as concentration of AKG in diluate solution
BC	—	Interaction between factors *B* and *C*
BPM	—	Bipolar membrane
C	—	Factor interpreted as the volume ratio of the concentrate to the diluate
CE	—	Current efficiency
C:*D*	—	Volume ratio of the concentrate to the diluate
EC	—	Energy consumption per 1 kg of AKG
EDBM	—	Electrodialysis with bipolar membrane
EDM	—	Electrodialysis metathesis
HPLC	—	High-performance liquid chromatography
N–P	—	Nernst–Planck
RSM	—	Response surface methodology

Symbols

A	—	Total area of anion-exchange membranes, m^2
C	—	Concentration (g/L) or (mol/m^3)
d	—	Desirability of a single outcome, –
D	—	Overall desirability, –
d_i	—	Diffusivity of *i* component, m^2/s
F	—	Faraday's constant, C
I	—	Current intensity, A
J_i	—	Molar flux of *i* component, mol/(m^2 s)
J_m	—	Average flux of AKG anions through the membrane, kg/(m^2 h)
m	—	Mass of the final product, g
n	—	Number of cell pairs, –
P	—	Pressure, MPa
R	—	Universal gas constant, J/(mol K)
R^2	—	Coefficient of determination, –
t	—	Time, s
T	—	Absolute temperature, K
U	—	Voltage, V
V	—	Diluate volume, mL
w_i	—	Weight of *i* response, –
y	—	Coordinate, m
z	—	Valence of ions, –
ΔC	—	Change of concentration in the diluate chamber, g/L
Δt	—	Change of time, s
η	—	Current efficiency, –
ϕ	—	Electric potential, V

Subscripts

AKG	—	Of AKG
diluate	—	In diluate
i	—	Response *i*
m	—	Membrane
T	—	Total

References

[1] Y. Wang, C. Huang, T. Xu, Which is more competitive for production of organic acids, ion-exchange or electrodialysis with bipolar membranes?, J. Membr. Sci., 374 (2011) 150–156.
[2] H. Nagasawa, A. Iizuka, A. Yamasaki, Y. Yanagisawa, Utilization of bipolar membrane electrodialysis for the removal of boron from aqueous solution, Ind. Eng. Chem. Res., 50 (2011) 6325–6330.
[3] Y. Wang, X. Zhang, T. Xu, Integration of conventional electrodialysis and electrodialysis with bipolar membranes for production of organic acids, J. Membr. Sci., 365 (2010) 294–301.
[4] R.C. Wu, Y.Z. Xu, Y.Q. Song, J.A. Luo, D. Liu, A novel strategy for salts recovery from 1,3-propanediol fermentation broth by bipolar membrane electrodialysis, Sep. Purif. Technol., 83 (2011) 9–14.
[5] V. Hábová, K. Melzoch, M. Rychtera, L. Přibyl, V. Mejta, Application of electrodialysis for lactic acid recovery, Czech J. Food Sci., 19 (2018) 73–80.
[6] T. Kurzrock, D. Weuster-Botz, Recovery of succinic acid from fermentation broth, Biotechnol. Lett., 32 (2010) 331–339.
[7] D. Pleissner, R. Schneider, J. Venus, T. Koch, Separation of lactic acid and recovery of salt-ions from fermentation broth, J. Chem. Technol. Biotechnol., 92 (2017) 504–511.
[8] P.A. Sosa, C. Roca, S. Velizarov, Membrane assisted recovery and purification of bio-based succinic acid for improved process sustainability, J. Membr. Sci., 501 (2016) 236–247.
[9] J. Antczak, M. Szczygiełda, K. Prochaska, An environment-friendly multi-step membrane-based system for succinic acid recovery from the fermentation broth, Desal. Water Treat., 128 (2018) 51–60.
[10] K. Prochaska, J. Antczak, M. Regel-Rosocka, M. Szczygiełda, Removal of succinic acid from fermentation broth by multistage process (membrane separation and reactive extraction), Sep. Purif. Technol., 192 (2018) 360–368.

[11] G. Box, S.J. Hunter, W.G. Hunter, Statistics for Experimenters: Design, Innovation, and Discovery, John Wiley & Sons, Inc., Hoboken, NJ, 2005.
[12] K. Hinkelmann, O. Kempthorne, Design and Analysis of Experiments, Volume 2: Advanced Experimental Design, John Wiley & Sons, Inc., Hoboken, NJ, 2005.
[13] D.C. Montgomery, Design and Analysis of Experiments, John Wiley & Sons, Inc., New York, NY, 2001.
[14] J. Antony, Design of Experiments for Engineers and Scientists, Elsevier, London, 2014.
[15] E.M. van der Ent, T.P.H. Thielen, M.A. Cohen Stuart, A. van der Padt, J.T.F. Keurentjes, Electrodialysis system for large-scale enantiomer separation, Ind. Eng. Chem. Res., 40 (2001) 6021–6027.
[16] Y. Wang, C. Huang, T. Xu, Optimization of electrodialysis with bipolar membranes by using response surface methodology, J. Membr. Sci., 362 (2010) 249–254.
[17] J.B. Severo Júnior, T.L.M. Alves, H.C. Ferraz, Removal of lactobionic acid by electrodialysis, Braz. J. Chem. Eng., 31 (2014) 1003–1011.
[18] L.M. Camacho, J.A. Fox, J.O. Ajedegba, Optimization of electrodialysis metathesis (EDM) desalination using factorial design methodology, Desalination, 403 (2017) 136–143.
[19] W. YaPing, R. Ben, Y. Hong, H. Rui, L. Li, L. Ping'an, M. Lixin, High-level expression of L-glutamate oxidase in *Pichia pastoris* using multi-copy expression strains and high cell density cultivation, Protein Expression Purif., 129 (2017) 108–114.
[20] M. Holz, C. Otto, A. Kretzschmar, V. Yovkova, A. Aurich, M. Pötter, A. Marx, G. Barth, Overexpression of alpha-ketoglutarate dehydrogenase in *Yarrowia lipolytica* and its effect on production of organic acids, Appl. Microbiol. Biotechnol., 89 (2011) 1519–1526.
[21] M. Szczygiełda, J. Antczak, K. Prochaska, Separation and concentration of succinic acid from post-fermentation broth by bipolar membrane electrodialysis (EDBM), Sep. Purif. Technol., 181 (2017) 53–59.
[22] K. Prochaska, K. Staszak, M.J. Woźniak-Budych, M. Regel-Rosocka, M. Adamczak, M. Wiśniewski, J. Staniewski, Nanofiltration, bipolar electrodialysis and reactive extraction hybrid system for separation of fumaric acid from fermentation broth, Bioresour. Technol., 167 (2014) 219–225.
[23] Y. Wang, Z. Zhang, C. Jiang, T. Xu, Recovery of gamma-aminobutyric acid (GABA) from reaction mixtures containing salt by electrodialysis, Sep. Purif. Technol., 170 (2016) 353–359.
[24] M. Szczygiełda, K. Prochaska, Alpha-ketoglutaric acid production using electrodialysis with bipolar membrane, J. Membr. Sci., 536 (2017) 37–43.
[25] M. Szczygiełda, K. Prochaska, Recovery of alpha-ketoglutaric acid from model fermentation broth using electrodialysis with bipolar membrane, Sep. Sci. Technol., 55 (2020) 165–175.
[26] M. Szczygiełda, K. Prochaska, Recovery of alpha-ketoglutaric acid from multi-component model solutions: impact of initial composition of diluate solution on the efficiency of the EDBM process, Desal. Water Treat., 128 (2018) 27–33.
[27] G. Derringer, R. Suich, Simultaneous optimization of several response variables, J. Qual. Technol., 12 (1980) 214–219.
[28] G.C. Derringer, A balancing act: optimizing a product's properties, Qual. Prog., 27 (1994) 51–58.
[29] M. Moresi, F. Sappino, Electrodialytic recovery of some fermentation products from model solutions: techno-economic feasibility study, J. Membr. Sci., 164 (2000) 129–140.
[30] T. Scarazzato, Z. Panossian, J.A.S.S. Tenório, V. Pérez-herranz, D.C.R.R. Espinosa, Water reclamation and chemicals recovery from a novel cyanide-free copper plating bath using electrodialysis membrane process, Desalination, 436 (2018) 114–124.
[31] M. Sadrzadeh, T. Mohammadi, Treatment of sea water using electrodialysis: current efficiency evaluation, Desalination, 249 (2009) 279–285.
[32] M.P. Mier, R. Ibañez, I. Ortiz, Influence of ion concentration on the kinetics of electrodialysis with bipolar membranes, Sep. Purif. Technol., 59 (2008) 197–205.
[33] M. Bailly, H. Roux-De Balmann, P. Aimar, F. Lutin, M. Cheryan, Production processes of fermented organic acids targeted around membrane operations: design of the concentration step by conventional electrodialysis, J. Membr. Sci., 191 (2001) 129–142.
[34] M.J. Woźniak, K. Prochaska, Fumaric acid separation from fermentation broth using nanofiltration (NF) and bipolar electrodialysis (EDBM), Sep. Purif. Technol., 125 (2014) 179–186.
[35] Y. Wei, C. Li, Y. Wang, X. Zhang, Q. Li, T. Xu, Regenerating sodium hydroxide from the spent caustic by bipolar membrane electrodialysis (BMED), Sep. Purif. Technol., 86 (2012) 49–54.

Supplementary information

Table S1
ANOVA for regression models, where: ***$p < 0.001$, **$p < 0.01$, *$p < 0.05$

	Current efficiency (%)						Energy consumption (kWh/kg)					
	DF	SS	MS	*F*-value	*p*-value	SGFNT	DF	SS	MS	*F*-value	*p*-value	SGFNT
A	1	1.25E+00	1.25E+00	8.03E+01	1.92E-05	***	1	9.49E-02	9.49E-02	7.42E+03	3.68E-13	***
B	1	4.43E+00	4.43E+00	2.85E+02	1.54E-07	***	1	3.70E-05	3.70E-05	2.91E+00	1.27E-01	
C	1	9.84E+00	9.84E+00	6.33E+02	6.67E-09	***	1	1.57E-04	1.57E-04	1.23E+01	8.06E-03	**
A:*B*	1	2.90E+01	2.90E+01	1.87E+03	9.06E-11	***	1	1.58E-03	1.58E-03	1.24E+02	3.80E-06	***
A:*C*	1	2.86E+00	2.86E+00	1.84E+02	8.36E-07	***	1	1.38E-04	1.38E-04	1.08E+01	1.12E-02	*
B:*C*	1	1.80E-02	1.80E-02	1.16E+00	3.13E-01		1	1.00E-05	1.00E-05	7.78E-01	4.04E-01	
A:*B*:*C*	1	8.46E-02	8.46E-02	5.44E+00	4.80E-02	*	1	4.00E-06	4.00E-06	2.82E-01	6.10E-01	
Residuals	8	1.24E-01	1.55E-02				8	1.02E-04	1.30E-05			
	Flux (kg/(m^2 h))						Time (min)					
	DF	SS	MS	*F*-value	*p*-value	SGFNT	DF	SS	MS	*F*-value	*p*-value	SGFNT
A	1	1.36E-01	1.36E-01	2.22E+04	4.57E-15	***	1	7.01E+02	7.01E+02	3.18E+04	1.09E-15	***
B	1	1.70E-05	1.70E-05	2.71E+00	1.39E-01		1	7.30E+02	7.30E+02	3.31E+04	9.29E-16	***
C	1	2.02E-04	2.02E-04	3.30E+01	4.32E-04	***	1	1.77E+00	1.77E+00	8.03E+01	1.92E-05	***
A:*B*	1	5.98E-04	5.98E-04	9.77E+01	9.26E-06	***	1	7.59E+01	7.59E+01	3.44E+03	7.91E-12	***
A:*C*	1	1.80E-05	1.80E-05	2.90E+00	1.27E-01		1	1.44E+00	1.44E+00	6.53E+01	4.05E-05	***
B:*C*	1	9.00E-06	9.00E-06	1.52E+00	2.53E-01		1	8.40E-01	8.40E-01	3.80E+01	2.70E-04	***
A:*B*:*C*	1	1.10E-05	1.10E-05	1.88E+00	2.08E-01		1	4.80E-01	4.80E-01	2.19E+01	1.58E-03	**
Residuals	8	4.90E-05	6.00E-06				8	1.80E-01	2.00E-02			

DF, degree of freedom; SS, the sum of squares; MS, mean square.